



**Cite this article:** Benabdallah NS, Gautier P, Hekimoglu-Balkan B, Lettice LA, Bhatia S, Bickmore WA. 2016 SBE6: a novel long-range enhancer involved in driving sonic hedgehog expression in neural progenitor cells. *Open Biol.* **6:** 160197. <http://dx.doi.org/10.1098/rsob.160197>

Received: 2 July 2016

Accepted: 20 October 2016

**Subject Area:**

developmental biology/genomics

**Keywords:**

sonic hedgehog, long-range enhancer, neural progenitor cells

**Author for correspondence:**

Wendy A. Bickmore

e-mail: [wendy.bickmore@igmm.ed.ac.uk](mailto:wendy.bickmore@igmm.ed.ac.uk)

Electronic supplementary material is available online at <https://dx.doi.org/10.6084/m9.figshare.c.3569433>.

# SBE6: a novel long-range enhancer involved in driving sonic hedgehog expression in neural progenitor cells

Nezha S. Benabdallah<sup>1,2</sup>, Philippe Gautier<sup>1</sup>, Betul Hekimoglu-Balkan<sup>1</sup>, Laura A. Lettice<sup>1</sup>, Shipra Bhatia<sup>1</sup> and Wendy A. Bickmore<sup>1</sup>

<sup>1</sup>MRC Human Genetics Unit, and <sup>2</sup>Edinburgh Super Resolution Imaging Consortium (ESRIC), Institute of Genetics and Molecular Medicine, University of Edinburgh, Crewe Road, Edinburgh EH4 2XU, UK

WAB, 0000-0001-6660-7735

The expression of genes with key roles in development is under very tight spatial and temporal control, mediated by enhancers. A classic example of this is the sonic hedgehog gene (*Shh*), which plays a pivotal role in the proliferation, differentiation and survival of neural progenitor cells both *in vivo* and *in vitro*. *Shh* expression in the brain is tightly controlled by several known enhancers that have been identified through genetic, genomic and functional assays. Using chromatin profiling during the differentiation of embryonic stem cells to neural progenitor cells, here we report the identification of a novel long-range enhancer for *Shh*—*Shh*-brain-enhancer-6 (SBE6)—that is located 100 kb upstream of *Shh* and that is required for the proper induction of *Shh* expression during this differentiation programme. This element is capable of driving expression in the vertebrate brain. Our study illustrates how a chromatin-focused approach, coupled to *in vivo* testing, can be used to identify new cell-type specific *cis*-regulatory elements, and points to yet further complexity in the control of *Shh* expression during embryonic brain development.

## 1. Introduction

Enhancers orchestrate the regulation of gene expression, which is critical for cell lineage specification and differentiation, and they therefore have a pivotal role during embryonic development [1]. A well-defined example of such *cis*-regulatory control is seen in the case of the sonic hedgehog (*Shh*) gene. *Shh* encodes a secreted signalling protein that imparts patterns of growth and identity to cells during many stages of embryonic development, including neural progenitors throughout ventral regions of the developing central nervous system (CNS) [2–4] (figure 1*a*).

*Shh* is located at one end of a large (approx. 1 Mb) regulatory domain containing a number of known enhancers controlling various *Shh* expression domains [5–12] (figure 1*b*). Precise *Shh* expression is critical for proper spinal cord and brain development, and this is governed by a subset of floor-plate and brain enhancers, many of which were identified by reporter assays. *Shh* floor-plate enhancer SFPE1, located 8 kb upstream of the *Shh* transcription start site (TSS), drives expression in the ventral spinal cord, and SFPE2 and *Shh*-brain-enhancer 1 (SBE1), positioned in the second intron of *Shh*, show activity in the floor plate of the spinal cord, as well as the ventral midbrain (mesencephalon), ventroposterior region of the diencephalon and the zona limitans intrathalamica (*zli*) [5,6]. An enhancer trap assay—using BAC transgenes to screen the *Shh* regulatory region—identified SBE2, SBE3 and SBE4 that drive *Shh* expression in the diencephalon (SBE2) and in the telencephalon (SBE4) [7]. Most recently, a combined informatics and experimental study identified SBE5 that drives expression in the *zli* [13].

Perturbation of *Shh cis*-regulation leads to severe neural defects in mammals. Translocations separating SBE2, 3 and/or 4 from *Shh*, disrupt the function of

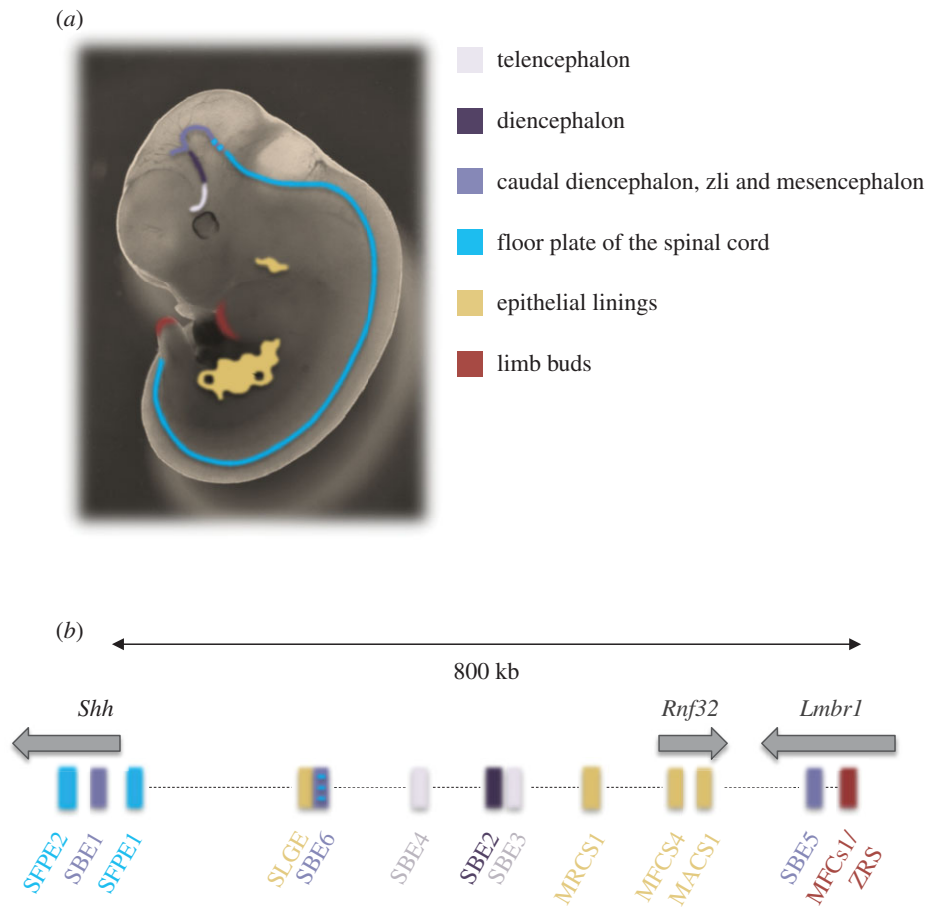


**Figure 1.** The sonic hedgehog (*Shh*) regulatory region. (a) Cartoon shows the sites of *Shh* enhancer activity in the E11.5 mouse embryo. Sites of *Shh* expression in the forebrain (telencephalon, diencephalon), caudal diencephalon, zli and midbrain/mesencephalon, floor plate, epithelial linings of gut and lung, and the distal limb bud are indicated with different colours. (b) Genomic map of the *Shh* regulatory region on mouse chromosome 5 indicating the known tissue-specific *Shh* enhancers, colour-coded as in (a).

these enhancers and lead to *Shh* haploinsufficiency, causing diverse holoprosencephaly (HPE) phenotypes [14,15], point mutation that results in the loss of SBE2 activity in the hypothalamus also leads to HPE [16]. Together, these observations highlight the importance of reporting and understanding new *cis*-regulatory elements that control *Shh* expression in the CNS.

Using chromatin profiling during the *in vitro* differentiation of mouse embryonic stem cells (mESCs) to neural progenitor cells (NPCs), we report a new *Shh* brain enhancer (SBE6) that we show is necessary for proper *Shh* expression in NPCs and that is active in vertebrate brain and neural tube development in transgenic assays.

## 2. Material and methods

### 2.1. Cell culture and neural differentiation

46c mouse embryonic stem cells (mESCs), derived from E14tg2A, contain a GFP insertion into the *Sox1* locus [17]. mESCs were cultured and differentiated into NPCs for 5 or 7 days with N2B27 medium as described previously [18]. To sort GFP<sup>+</sup> cells after transfection or differentiation, cells were trypsinized and resuspended in PBS + 10% medium. Flow cytometric analysis was performed, using the 488 nm laser of a BD FACSAriaII SORP (Becton Dickinson) with 525/50 nm bandpass filters. BD FACSDIVA software (Becton Dickinson, v. 6.1.2) was used for instrument control and data analysis.

### 2.2. Quantitative analysis of gene expression

RNA was prepared from approximately  $1 \times 10^6$  46c mESCs or NPCs, using the RNeasy mini kit (Qiagen) according to the manufacturer's protocol, including a DNaseI (Qiagen) treatment for 15 min at room temperature. cDNA was synthesized from 2  $\mu$ g purified RNA with superscript II reverse transcriptase (Invitrogen) primed with random hexamers (Promega). Real-time (q)PCR was carried out on a Roche LightCycler 480 real-time PCR system, using a LightCycler 480 Sybr Green detection kit (Roche) as described previously [19]. Primer pairs for qRT-PCR are listed in electronic supplementary material, table S1.

The real-time thermal cycler was programmed as follows: 15 min Hotstart; 44 PCR cycles (95°C for 15 s, 55°C for 30 s, 72°C for 30 s). The relative mRNA expression for each primer set in each sample was measured by the LIGHTCYCLER software and normalized to the mean for *Gapdh* from at least two biological replicates and technical triplicates.

### 2.3. Native chromatin immunoprecipitation and microarray analysis

Nuclei from  $3 \times 10^6$  mESCs or sorted Sox1+ NPCs were prepared and resuspended in NB-R (85 mM NaCl, 5.5% sucrose, 10 mM Tris-HCl pH 7.5, 3 mM MgCl<sub>2</sub>, 1.5 mM CaCl<sub>2</sub>, 0.2 mM PMSF, 1 mM DTT) as previously described [20]. Micrococcal nuclease (MNase) digestion and native chromatin

immunoprecipitation (ChIP) were performed as previously described [21,22]. Antibodies used for ChIP were H3K4me1 (Abcam ab8895) and H3K27ac (Millipore 07-360).

Ten nanograms (optimal) of input or ChIP DNA were amplified, using the WGA2 whole genome amplification kit (Sigma). Amplified material was labelled with Cy3 or Cy5 by random priming according to the NimbleGen ChIP-chip protocol (Roche). In total, two or three biological replicates with dye swaps were hybridized for 20 h and washed according to the manufacturer's protocol. A custom  $3 \times 720$  K mouse tiling array (NimbleGen, Roche) containing 179 493 unique probes from different genomic regions was used, with each probe represented by four replicates. Arrays were scanned on a NimbleGen MS 200 Microarray scanner (Roche), using 100% laser power and 2  $\mu$ m resolution. Raw signal intensities were quantified from TIFF images, using MS 200 DATA COLLECTION software.

Microarray data were analysed in R, using the bioconductor packages BEADARRAY and LIMMA according to the Epigenesis NimbleGen ChIP-on-chip protocol 43 ([www.epigenesis.eu/en/protocols/bioinformatics](http://www.epigenesis.eu/en/protocols/bioinformatics)). Scale normalization was used within replicates, to control interarray variability. Each condition was represented by two biological replicates hybridized as dye swap experiments and enrichment scores are defined as  $\log_2$  ChIP/input signal.

## 2.4. Computational analysis of the SBE6 region

Evolutionary conservation of the SBE6 region was assessed, using the 'Vertebrate Multiz Alignment & Conservation/Multiz Alignments and Conserved Elements' tracks in the UCSC genome browser [23]. This delineated the following subregions for further analysis:

SBE6.1: Chr5: 28 889 688–28 890 461, SBE6.2: Chr5: 28 893 935–28 895 000 (mm9)

R<sub>VISTA</sub> [24] was used to align the mouse and human orthologous sequences, with the default sequence aligner (LAGAN) and default parameters. Transcription factor binding sites (TFBS) for known forebrain transcription factors [25] available on the R<sub>VISTA</sub> server were selected (Arx, Maf, Dlx5, Pbx1, ER81, Six3, Vax1).

JASPAR [26] was used independently on the mouse and human core sequences, searching for potential neural activity present in the Jaspar Core Vertebrata matrices list (DLX6, PBX1, ETV1, Six3, SP8 and VAX1) with the default parameters (relative profile score threshold 80%; electronic supplementary material, table S2). Hits were then highlighted on the R<sub>VISTA</sub> alignment.

## 2.5. Zebrafish enhancer reporter assay

The putative SBE6.1 and SBE6.2 enhancers were cloned by PCR amplification of the relevant fragment and flanking sequence from mouse genomic DNA, using Phusion high fidelity polymerase (NEB) and the following primers:

Sbe6.1 Fw B4: **AGGGGAGA**ACTTTGTATAGAAAAGTTG  
GCGCGCCACCTGCTTCTCTGAGGAA

Sbe6.1 Rv B1R: **AGGGGACTG**CTTTTTTGTACAAACTTG  
CTTAGGCCATTGTGCCAC

Sbe6.2 Fw B4: **AGGGGAGA**ACTTTGTATAGAAAAGTT  
GCGCGCTGAAGTCAAGGGCTGGTACT

Sbe6.2 Rv B1R: **AGGGGACTG**CTTTTTTGTACAAACT  
TGATCAGCCCTCCAGTTTGACT

Negative controls used were sequences 3' of *Shh*, which have no suspected regulatory activity, and which are the same genomic distance from *Shh* as SBE6.1 and SBE6.2 are upstream (5') of *Shh*.

Negative controls:

Sbe6.1 Fw B4: **AGGGGAGA**ACTTTGTATAGAAAAGTT  
GCGCGCCGAGTGCAGGTGTTTGTGAA

Sbe6.1 Rv B1R: **AGGGGACTG**CTTTTTTGTACAAACTT  
GCCTCAACACAGCATTGCCAA

Sbe6.2 Fw B4: **AGGGGAGA**ACTTTGTATAGAAAAGTT  
GCGCGCAGAGAGTGAAGATTCCAGCT

Sbe6.2 Rv B1R: **AGGGGACTG**CTTTTTTGTACAAACTT  
GTGAGGCAGTGTCTATCTTTTGAC

attB4 and attB1r sequences (bold) were included in the PCR primers for use with the Gateway recombination cloning system (Invitrogen, 12538120). The amplified fragment was first cloned into the Gateway pP4P1r entry vector and sequenced using M13 forward and reverse primers for verification. The elements in the pP4P1r vector were combined with a pDONR221 construct containing either a Gata2 promoter-eGFP- polyA or a Gata2 promoter mCherry-polyA cassette [27], and recombined into a destination vector with a Gateway R4-R2 cassette flanked by Tol2 recombination sites.

Reporter plasmids were isolated using Qiagen miniprep columns and were further purified using a Qiagen PCR purification column (Qiagen), and diluted to 50 ng  $\mu$ l<sup>-1</sup> with DNase/RNase free water. Tol2 transposase RNA was synthesized from a *NotI*-linearized pCS2-TP plasmid using the SP6 mMessage mMachine kit (Ambion), and similarly diluted to 50 ng  $\mu$ l<sup>-1</sup>. Equal volumes of the reporter construct(s) and the transposase RNA were mixed immediately prior to injections. 1–2 nl of the solution was microinjected per zebrafish embryo at the one- to two-cell stage for up to 200 embryos. Embryos were screened for fluorescence at 1–5 days post-fertilization (i.e. 24–120 hours post-fertilization, hpf) and raised to adulthood. Germline transmission was identified by mating of sexually mature adults to wild-type fish and examining their progeny for fluorescence. F<sub>1</sub> embryos from three to five F<sub>0</sub> lines showing the best representative expression pattern for each construct were selected for confocal imaging. A few positive embryos were also raised to adulthood, and F<sub>1</sub> lines were maintained by outcrossing. A summary of the independent lines analysed for each construct and their expression sites is included in electronic supplementary material, table S3. Imaging of zebrafish reporter transgenic embryos was carried out as previously described [27].

## 2.6. Mouse transgenic reporter assays

The same SBE6.1 PCR amplicon, with attB4 and attB1r sequences included as used for reporter assays in zebrafish (above), were used to generate enhancer-reporter constructs for mouse transgene assays. The amplicon was cloned directly into an hsp68-LacZ vector containing a P4-P1r entry cassette [28]. Transgenic mice were generated by microinjection into mouse oocytes, and the analysis of transgenic lines was carried out as previously described [28]. Two independently derived E11.5 SBE6.1-LacZ embryos were independently analysed; one a transient insertion, the second from a stable line. For analysis, embryos were dissected in PBS and left in LacZ fix for 1 h (1% formaldehyde; 0.2% glutaraldehyde; 2 mM

MgCl<sub>2</sub>; 5 mM EGTA; 0.02% NP-40 in PBS). After fixation the embryos were washed in PBS containing 0.02% NP-40, before being stained overnight at 37°C in the dark in a solution containing 5 mM K<sub>3</sub>Fe(CN)<sub>6</sub>; 5 mM K<sub>4</sub>Fe(CN)<sub>6</sub>·3H<sub>2</sub>O; 2 mM MgCl<sub>2</sub>; 0.01% sodium deoxycholate; 0.02% NP-40 and 0.1% 5-bromo-4-chloro-3-indolyl-β-D-galactopyranoside (X-gal). Embryos were then fixed with 4% PFA and photographed on a Leica MZ FLIII Microscope fitted with a Hamamatsu Orca-ER digital camera and a CRI microcolour filter.

## 2.7. mRNA *in situ* hybridization

RNA *in situ* hybridization on fish embryos was performed as previously described [29]. The sequences of primers used for synthesis of *Shh* hybridization probes are the following:

Forward primer (5'-SP6 promoter-sequence-3') AAGCTGACACCTCTCGCCTA and reverse primer (5'-T7 promoter-sequence-3') GAGCAATGAATGTGGGCTTT.

Mouse *in situ* hybridization was performed with DIG-labelled gene-specific antisense probes as previously described [30]. The *Shh* probe was provided by McMahon [31].

## 2.8. Deletion of SBE6 from the 46c embryonic stem cell genome

Cell line deletions were produced, using the Crispr/cas9 system. SBE6.1- and SBE6.2-specific gRNA primers (electronic supplementary material, table S4) were cloned into the cas9 plasmid pX458 following protocols from the Zhang laboratory [32–34]. 46C mESCs were transfected with the resulting plasmids using Lipofectamine 2000 reagent (Invitrogen cat. no. 11668) following the manufacturer's recommendations as described in [19]. Single transfected cells were sorted based on GFP expression from pX458 and cultured further. DNA extraction and genotyping were performed 7 days after sorting, using overnight incubation at 55°C with lysis buffer (10 mM TrisHCl pH 7.5, 10 mM EDTA, 10 mM NaCl, 0.5% SDS, 1 mg ml<sup>-1</sup> ProteinaseK) followed by ethanol precipitation and washes. Genomic DNA was amplified with the following primers:

SBE6.1 Fw: TTTTGGGAAGCTTAAATGCCCAT  
 SBE6.1 Rv: CCACCACAAGCACATTCAT  
 SBE6.2 Fw: GCCTCCATGAAGTCCAATGG  
 SBE6.2 Rv: CCACCCTTGCTACTCAGGAA

Amplification was done using DreamTaq Green PCR master mix (ThermoFisher K1081) following the manufacturer's protocol and PCR products were assessed by agarose gel electrophoresis. Amplified products were later sequenced to further confirm homozygous deletions.

## 3. Results

### 3.1. SBE6.1 and SBE6.2, two new putative *cis*-regulatory elements active in neural progenitor cells

We used the differentiation of 46c mESCs as a model system to identify putative regulatory elements that may become activated concomitant with the expression of *Shh* during neural differentiation. These cells contain a knockin of GFP into the *Sox1* locus allowing for the monitoring of neural

differentiation and the purification, by fluorescence-activated cell sorting (FACS), of Sox1+ neuroepithelial progenitor cells (NPCs; figure 2a) [17,35,36]. Sox1+ cells appear after day 3 of differentiation, and from day 3 to 7, expression of *Shh* and *Nestin* increase while *Oct4* mRNA levels progressively decrease (figure 2b). Analysis of these NPC cells for expression of markers from different regions of the developing brain (figure 2c) suggests that these cells do not have a distinct regional identity, though there is some evidence for a slight shift towards a more telencephalic fate (increasing *Six3* and *Emx2* expression) and away from the hindbrain (decreasing *En2* and *Gbx2* expression) by day 7 (figure 2d).

Genome-wide ChIP has allowed the identification of several post-translational histone modification characteristics of active enhancers including H3K4me1 and H3K27ac [37]. The use of these two histone marks is widely employed to identify new active enhancer elements in the genome [38], though they are not comprehensive [18,39]. Using native ChIP coupled to hybridization on microarrays (ChIP-chip) that tile the whole *Shh* regulatory region, we assessed the sites of enriched H3K4me1 and H3K27ac in mESCs (where *Shh* is not expressed) and in Sox1+ NPC after 5 days of neural differentiation. Significant gains of H3K4me1 and H3K27ac were not detected at the known SBE2, 3, 4 or 5 brain enhancers (figure 3a). However, a prominent change in the ChIP profile was seen at a small region approximately 100 kb upstream of the *Shh* TSS. This region has no evidence of active enhancer marks in mESCs but gains both H3K4me1 and H3K27ac upon neural differentiation (figure 3a).

Analysis of sequence conservation across multiple vertebrate species indicated that this region contains two blocks of evolutionary conservation in mammals and birds, and we named these putative NPC enhancers SBE6.1 (mm9 coordinates Chr5: 28 889 688–28 890 461, 96 048 bp upstream of *Shh* TSS) and SBE6.2 (Chr5: 28 893 935–28 895 000, 100 295 bp away from *Shh*; figure 3b). Interestingly, two other sequences beyond SBE3 also show a gain of active enhancer marks (arrowheads in figure 3a), but are not investigated further here.

*In silico* motif analysis using UCSC comparative genomics of SBE6.1 and SBE6.2 allowed us to identify two core (approx. 1 kb) regions that are highly conserved. Complementary rVISTA, JASPAR and RSAT scans of those regions revealed the presence of predicted binding sites for neural transcription factors such as ETV1, SP8, VAX1 and DLX6 (electronic supplementary material, table S2).

The SBE6.1 sequence is entirely included in a recently described 1.7 kb lung and gut epithelium regulatory element for *Shh* expression in mouse embryos called SLGE (chr5: 28 889 230–28 890 979) [40], raising the possibility either that this enhancer has multiple regulatory activities or that SLGE is ectopically activated in NPCs. SBE6.2 has not previously been identified or studied.

### 3.2. SBE6.1 drives expression in the brain of developing zebrafish and mouse embryos

To test the regulatory potential of SBE6.1 and SBE6.2, we used a zebrafish Tol2 transposon assay in which the test element is juxtaposed to a minimal promoter driving the expression of either GFP or mCherry reporter gene expression. This assay has been shown to recapitulate the correct expression pattern for the SBE2 enhancer and to detect the loss of this enhancer activity

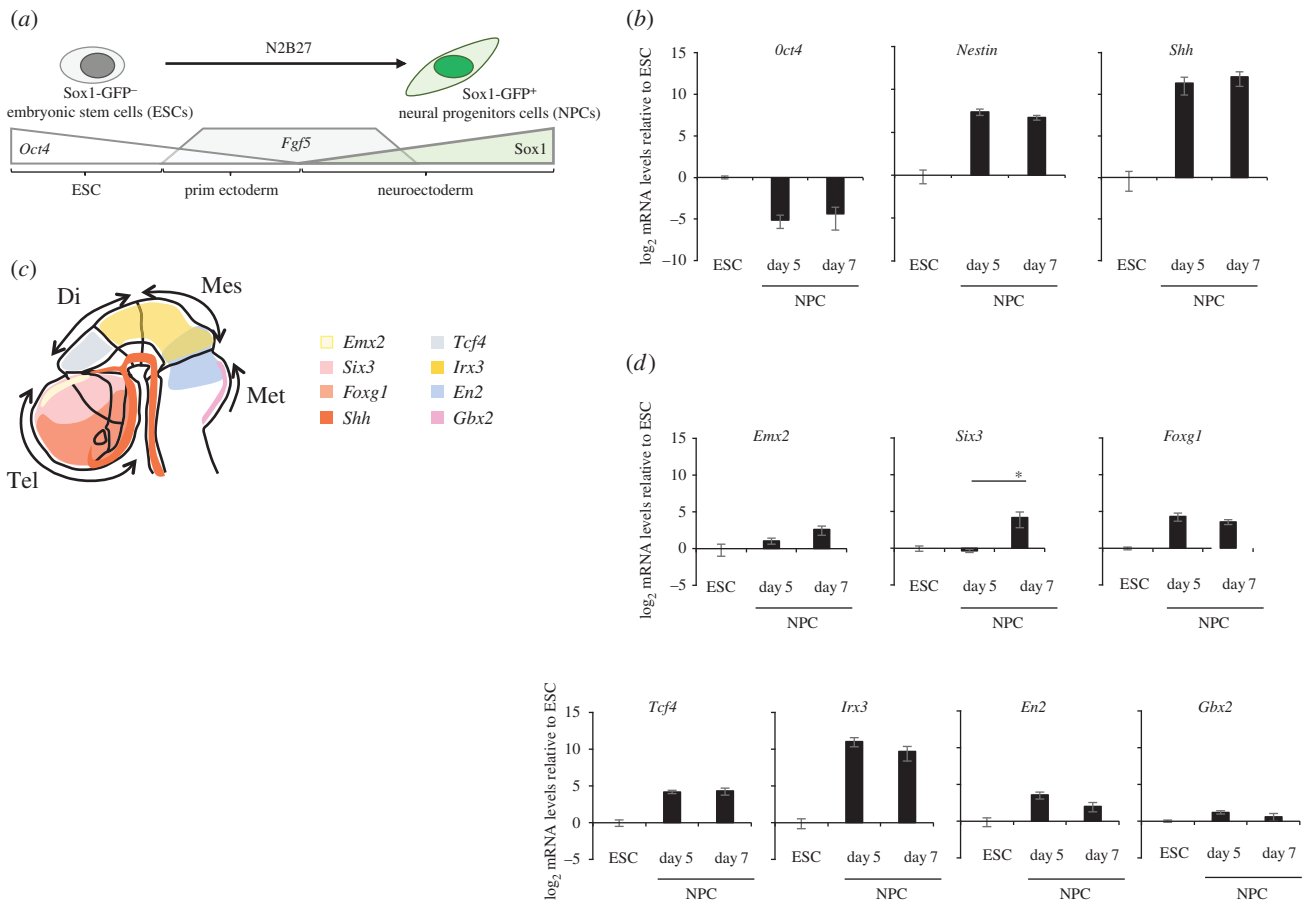


**Figure 2.** Sox1-GFP<sup>+</sup> neural differentiation from ESC to NPCs. (a) Schematic shows the differentiation of 46c mouse embryonic stem cells (ESC)—which are Sox1-GFP<sup>-</sup> and express high levels of the pluripotency factor *Oct4*—into first primitive ectoderm as *Oct4* levels decrease and fibroblast growth factor 5 (*Fgf5*) levels rise, and then further into neuroectoderm as *Fgf5* levels start to decrease and *Sox1* levels rise, allows for the purification of Sox1-GFP<sup>+</sup> neural progenitor cells (NPC). (b) qRT-PCR showing mean  $\pm$  s.e. of the mean (s.e.m.)  $\log_2$  mRNA levels for *Oct4*, *Nestin* and *Shh* in ESCs and in NPCs after 5 and 7 days of differentiation. Expression levels are relative to *Gapdh* and normalized to ESC mRNA levels. Data are from three biological replicates and technical triplicates. (c) Schematic of an E11.5 mouse brain and gene expression markers patterning the telencephalon (tel), diencephalon (di), mesencephalon (mes) and metencephalon (met). (d) qRT-PCR shows means ( $\pm$  s.e.m.) of  $\log_2$  mRNA levels of marker genes for different brain regions in ESC and NPC differentiated for 5 or 7 days. As in (b), levels are relative to *Gapdh* and normalized to ESC mRNA levels. *Six3* mRNA levels significantly increase in NPCs between days 5 and 7 of differentiation (one-tailed Student's *t*-test;  $p = 0.023$ ). Data consist of five biological replicates and technical triplicates.

associated with mutation of a SIX3 binding site found in the cases of HPE [16,27]. *In situ* hybridization for *Shh* mRNA in wild-type zebrafish embryos reveals expression in the forebrain at 48 and 72 hpf [27]. Using this assay, SBE6.1 enhancer activity was detected in the developing forebrain of the zebrafish embryos in four independent stable transgenic lines from 30 to 72 hpf (figure 4a,b; electronic supplementary material, table S3). SBE6.2 however failed to consistently drive reporter gene expression in the forebrain, with forebrain-specific activity noted in only one out of the four independent transgenic lines generated (electronic supplementary material, table S3). Therefore, SBE6.1 has a consistent enhancer function and is active in zebrafish forebrain development.

The ability of SLGE to drive expression in the developing mouse brain is unclear, but it is known to be capable of driving expression in the brain of transgenic rabbits [40]. We therefore made mouse transgenics to analyse the regulatory potential of SBE6.1 in mouse development. LacZ staining of transient and stable SBE6.1 transgenic embryos revealed activity in the pharyngeal endoderm, gut and cloaca of the mouse embryo as expected owing to the overlap with SLGE (electronic supplementary material, figure S1a,b). X-gal staining could be also detected in few superficial diencephalon cells where

*Shh* is not expressed (figure 4c; electronic supplementary material, figure S1c). However, SBE6.1 also showed activity in the developing ventral mesencephalon with some cells expressing SBE6-LacZ near the hindbrain and as well as in the ventral midline of the mouse embryonic neural tube—all sites of endogenous *Shh* expression (figure 4d,e; electronic supplementary material, figure S1d).

SBE6.1 is only active in a small number of cells in transgenic embryos, and we cannot at this stage confirm how accurately this recapitulates a subset of endogenous *Shh* expression. However, the strong similarities between the two mouse embryos do support our conclusion that the SBE6.1 enhancer is capable of activity in the developing vertebrate brain, from a forebrain pattern in zebrafish transgenics to a floor plate and ventral mesencephalon expression in mouse transgenic embryos.

### 3.3. SBE6.1 enhances *Shh* expression in neural progenitor cells

To determine the regulatory activity of SBE6.1 and SBE6.2 in their native context, we used CRISPR/Cas9 to delete these elements from the genome in 46c mESCs (SBE6.1<sup>-/-</sup> and

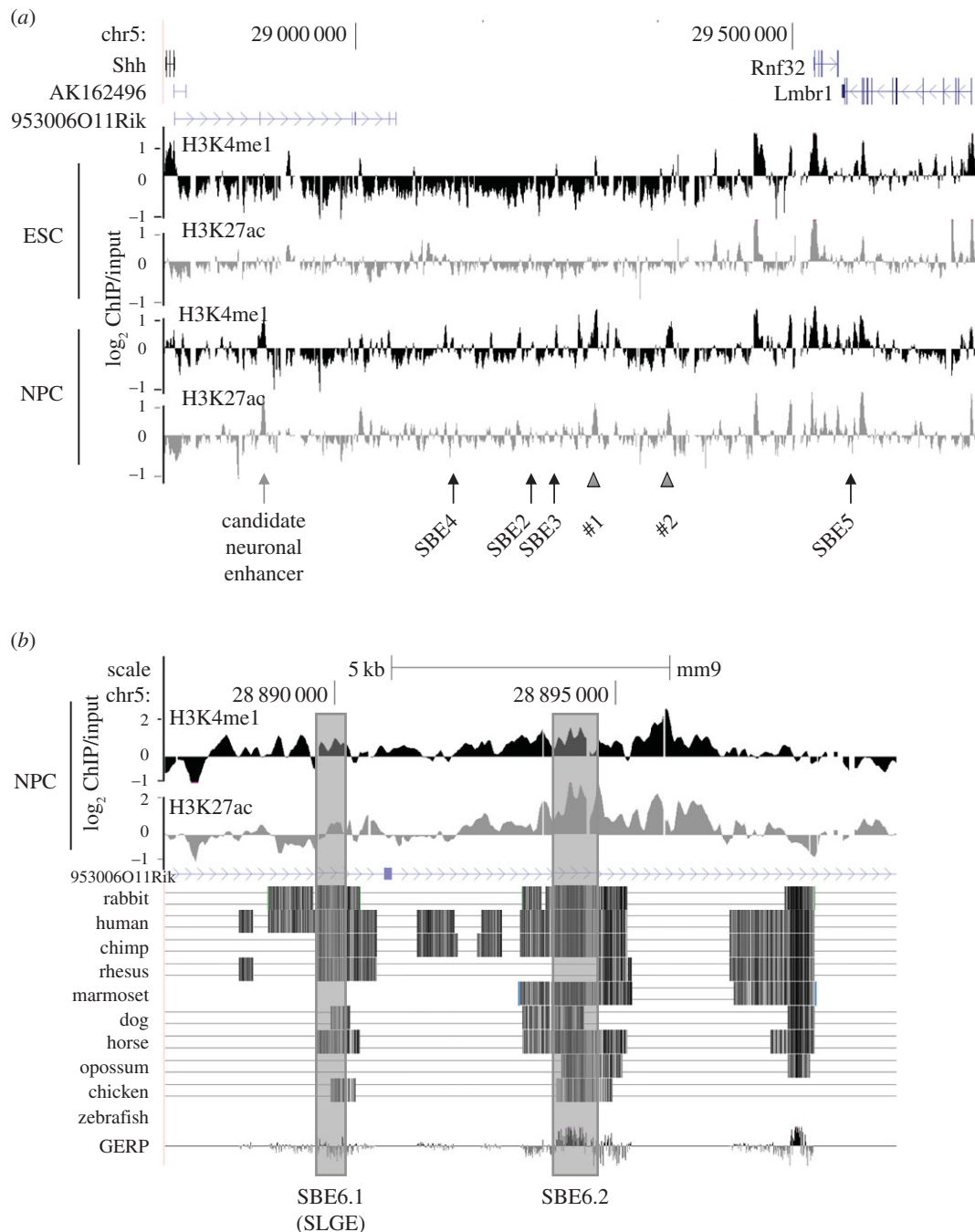


**Figure 3.** Chromatin immunoprecipitation analysis during NPC differentiation. (a)  $\log_2$  native ChIP/input MNase-digested chromatin for H3K4me1 (black) and H3K27ac (grey) from ESCs and Sox1<sup>+</sup> NPCs purified after 5 days of differentiation. Averages of data from two biological replicates are shown. The position of genes (above) and known neural enhancers for *Shh* (below) are shown; grey arrow indicates the new candidate neural enhancer SBE6; grey arrowheads indicate two other regions that gain active enhancer signatures in NPCs. Genome coordinates are from the mm9 assembly of the mouse genome (chr5: 28 782 000–29 711 000 bp). (b) Zoom-in of the region (chr5: 28 887 000–28 900 000) of putative NPC enhancer activity shows conservation across multiple vertebrate species. Two smaller core conserved regions named SBE6.1 (=SLGE) and SBE6.2 are indicated.

SBE6.2<sup>-/-</sup>; electronic supplementary material, figure S2). We generated and analysed two SBE6.1<sup>-/-</sup> and three SBE6.2<sup>-/-</sup> independent cell lines. Upon NPC differentiation, the proportion of Sox1-GFP<sup>+</sup> cells remained the same between NPCs derived from wild-type and SBE6.1<sup>-/-</sup> or SBE6.2<sup>-/-</sup> cells, analysis of *Oct4* and *Nestin* mRNA expression confirmed that differentiation of mESCs into NPC was not perturbed by the loss of either SBE6.1 or SBE6.2 (figure 5a). However, in NPCs derived from SBE6.1<sup>-/-</sup> but not SBE6.2<sup>-/-</sup> cells, levels of *Shh* expression were significantly reduced compared with wild-type cells (one-tailed Student's *t*-test;  $p = 0.002$ ). Average *Shh* mRNA levels in NPCs differentiated from

SBE6.2<sup>-/-</sup> ESCs were not significantly different relative to wild-type (figure 5b).

Together, these data suggest that SBE6.1 is a long-range enhancer that contributes to driving *Shh* expression during the differentiation of ESCs to neural progenitor cells.

## 4. Discussion

The regulation of *Shh* is a paradigm for the complex control of gene expression at different times and places in development. More than 10 discrete enhancers have been identified in the

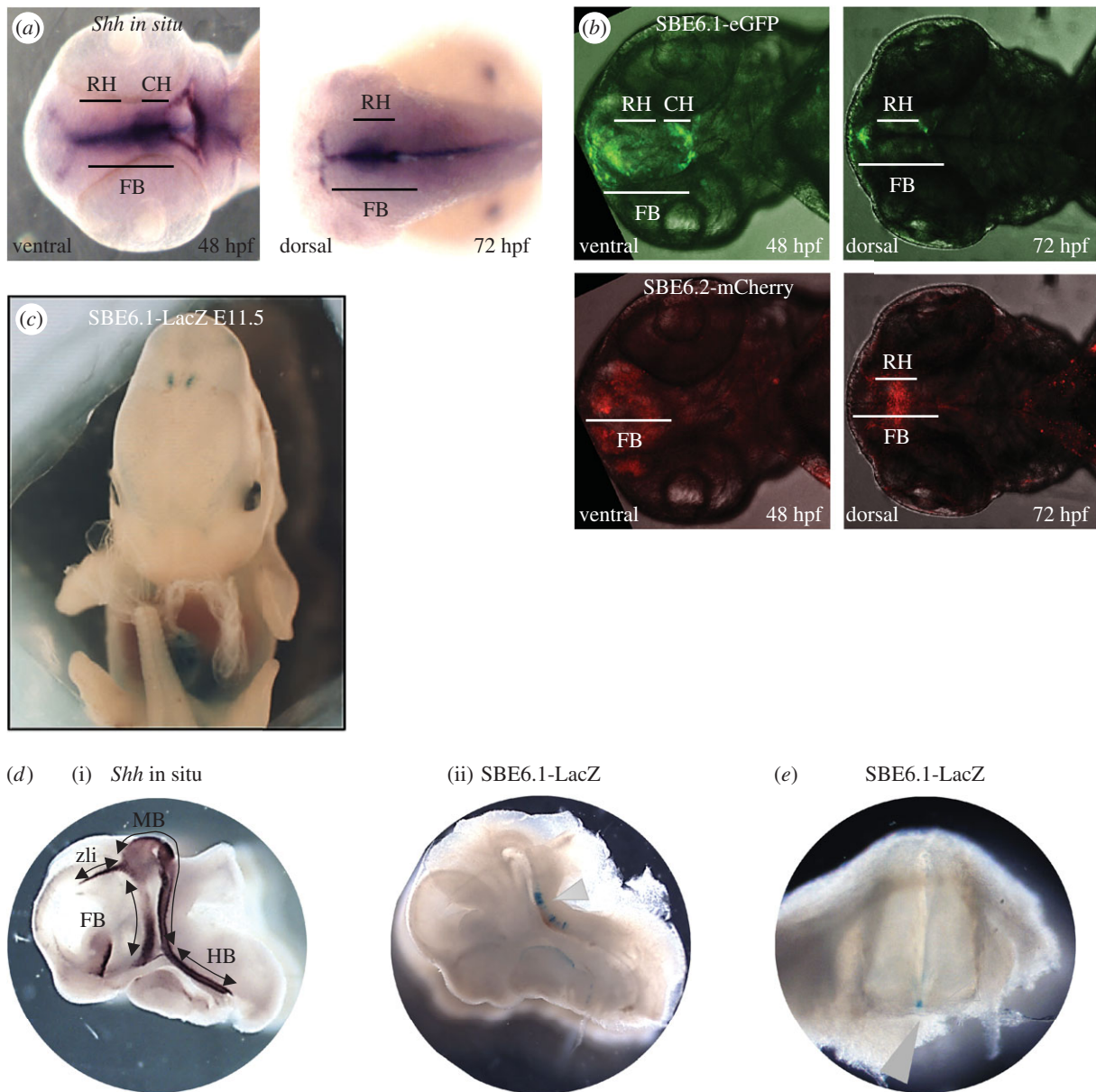


**Figure 4.** Enhancer reporter assays for SBE6.1 and SBE6.2. (a) *Shh* mRNA *in situ* hybridization on zebrafish embryos. A ventral view is shown at 48 h post-fertilization (hpf) and a dorsal view at 72 hpf. *Shh* expression is detected in the rostral hypothalamus (RH) and caudal hypothalamus (CH) of the forebrain (FB). (b) Confocal microscopy of 48 and 72 hpf zebrafish embryos from stable transgenic lines carrying a Tol2 transposon with SBE6.1 and SBE6.2, driving GFP and mCherry, respectively. Reporter gene expression is detected in the rostral hypothalamus (RH) and caudal hypothalamus (CH) of the forebrain (FB). (c) External view of the LacZ staining in a stable SBE6.1 transgenic E11.5 embryos shows expression in a portion of diencephalon cells. (d) (i) *Shh* mRNA *in situ* hybridization in an E11.5 mouse embryo displaying expression in the forebrain (telencephalon, diencephalon; FB), midbrain (caudal diencephalon, zona limitans intrathalamica (zli) and mesencephalon; MB), and hindbrain (HB). (ii) sagittal section of an E11.5 transient SBE6.1-LacZ transgenic embryo with arrowhead indicating staining in a portion of the ventral mesencephalon, with some cells expressing SBE6.1 near the hindbrain. (e) E11.5 transient SBE6.1-LacZ transgenic embryo with arrowhead indicating staining in the floor plate of the spinal cord.

large (approx. 1 Mb) *Shh* regulatory domain [12] (figure 1b). Most of these enhancers were identified using transgenic reporter assays [7]. Others have been identified through genetics in mouse and man when mutations in *Shh* enhancers cause phenotypes that result from aberrant control of specific aspects of *Shh* expression in development. Most recently, information on transcription factor motifs in known *Shh* brain enhancers has been used to search for other similar patterns of motifs in the *Shh* regulatory domain and has identified a new enhancer that drives *Shh* expression in a discrete region of the brain [7,13].

Here, we show that analysis of histone modifications (H3K4me1 and H3K27ac), typically associated with active enhancers, in an *in vitro* neural differentiation system can

be used to identify a new enhancer that is important for the activation of *Shh* in neural progenitor cells. This enhancer, which we have named SBE6, is located 100 kb 5' of *Shh* and is activated during the differentiation of mESCs to Sox1+ NPCs. Analysis of transcription factor motifs suggests that SBE6 contains consensus binding sites for a number of transcription factors expressed in the brain. Using an enhancer reporter assay in zebrafish and mouse, we show that *in vivo* the SBE6.1 region of SBE6, but not SBE6.2, can drive expression in the developing brain. Consistent with this, genetic ablation of SBE6.1 in mESCs, but not SBE6.2, abrogates the induction of *Shh* expression during *in vitro* NPC differentiation. Therefore, despite the presence of strong active enhancer histone modifications in NPCs, we find no

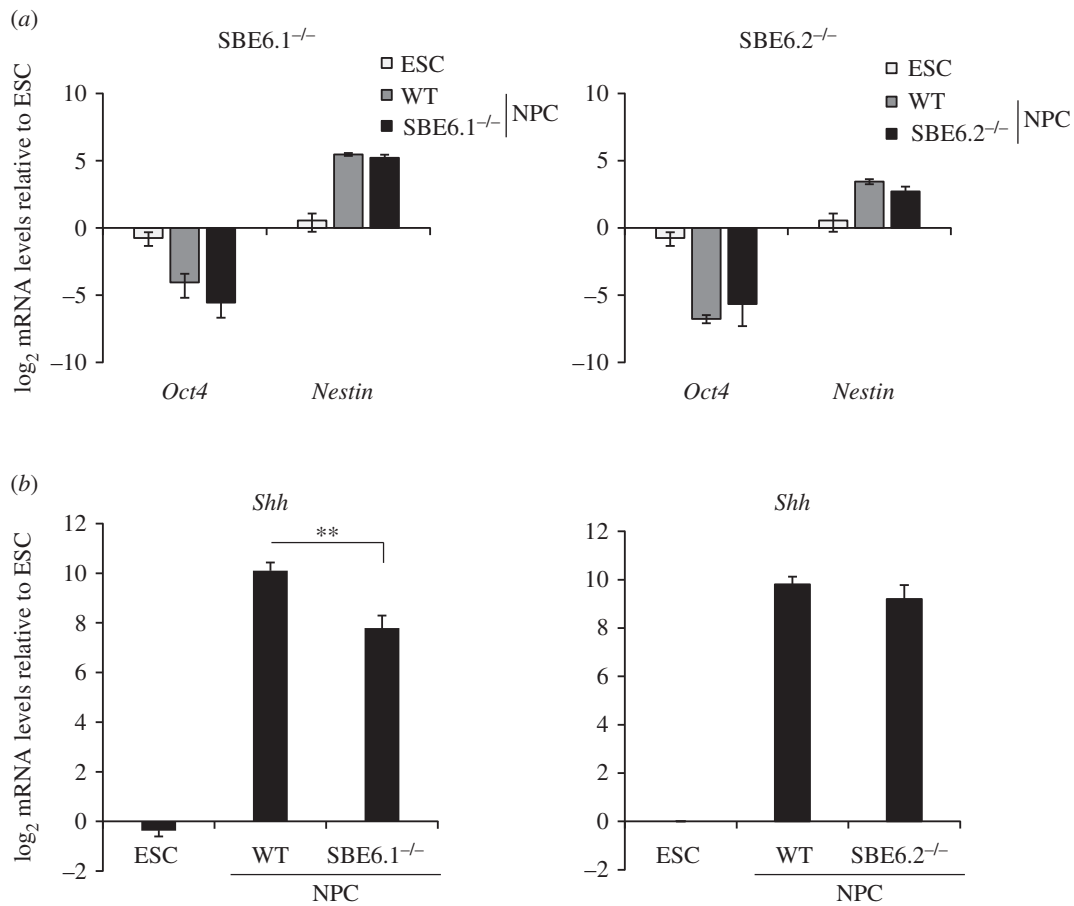


**Figure 5.** *Shh* expression levels in neural precursor cells (NPC) derived from ESC lines with SBE6.1 or SBE6.2 deletions. (a) qRT-PCR shows mean ( $\pm$  s.e.m.)  $\log_2$  mRNA levels of *Oct4* and *Nestin* in wild-type 46c ESC, and NPCs, and in NPCs derived from SBE6.1<sup>-/-</sup> (left) or SBE6.2<sup>-/-</sup> (right) 46c cells. Levels are relative to *Gapdh* and normalized to levels in wild-type ESCs. (b) As in (a) qRT-PCR shows mean ( $\pm$  s.e.m.)  $\log_2$  *Shh* mRNA levels in wild-type NPCs, and in NPCs derived from 46c cell lines deleted for SBE6.1 (left) or SBE6.2 (right). mRNA levels are shown relative to *Gapdh* and normalized to those in wild-type ESCs. *Shh* mRNA levels are significantly reduced in NPCs derived from SBE6.1<sup>-/-</sup> cell lines after 7 days of differentiation (one-tailed Student's *t*-test; *p*-value = 0.002). ESC data consist of three biological replicates, SBE6.1<sup>-/-</sup> dataset are six biological replicates from two independent deletion cell lines compared with six biological replicates of wild-type (WT) NPC. SBE6.2<sup>-/-</sup> data are from three biological replicates from three independent deletion cell lines with three biological replicates of wild-type (WT) NPCs.

functional evidence that SBE6.2 is a neural enhancer, highlighting that precise annotation and understanding of regulatory regions of the genome requires confirmation via functional enhancer assays.

Our analyses presented here add to the growing number of functionally validated enhancers directing *Shh* expression in different developmental contexts. Given the large size of the gene desert upstream of *Shh*, where many of these enhancers are located, there is the potential for this region to harbour many more *cis*-regulatory elements and, given the complexity of brain development, many of these may be enhancers active in the brain. Indeed, regulatory segmentation built from ChromHMM or Segway using ENCODE data from various mouse primary tissues indicates the presence of several regions with chromatin signatures indicative of enhancer activity in mouse brain at E14.5—a period of mouse development when neurogenesis is ongoing (figure 6a). This includes the genomic regions containing the known neural enhancers SBE2–4, but also a region that corresponds to SBE6. The many other regions called as likely active enhancers using the analysis from just four tissues (brain, liver, spleen and kidney) at one embryonic stage (figure 6a) suggests that the *Shh* regulatory region may harbour many tens of as yet unannotated enhancers. We note that the new sites detected by these high-throughput methods (marked with arrowheads as #1 and #2 in figure 6a) correspond

to peaks of H3K4me1/H3K27ac that are induced during the differentiation of 46c mESCs to NPCs (figures 3 and 6a; electronic supplementary material, figure S3). A similar analysis of chromatin profiling data from the Roadmap project also indicates the signature of an active neural enhancer at the position of SBE6 in material from different regions of the human brain and particularly in ganglionic eminence derived neurospheres (figure 6b). This analysis also indicates many other potential regulatory elements active in different brain regions.

It is interesting that the genome coordinates of SBE6.1 are completely contained within those reported for the *Shh* lung and gut epithelium regulatory element SLGE [40]. Transgenic analysis in the rabbit had shown that the mouse SLGE fragment can drive expression in the rabbit brain [40]. Here, we have shown that SBE6.1 can drive expression in the brain of zebrafish and mouse. Although we cannot completely exclude that our observations of SBE6.1 transgenic reporter expression in the vertebrate brain and neural tube represents ectopic activity of SLGE in these assays, our chromatin profiling indicates that this region does harbour active regulatory potential in Sox1+ NPCs. Consistent with this, ENCODE and Roadmap data also indicate that this region of the mammalian genome has active enhancer chromatin marks in neural tissue, as well as in the liver (figure 6a; electronic supplementary material, figure S3) and gastric tissue (figure 6b). Important



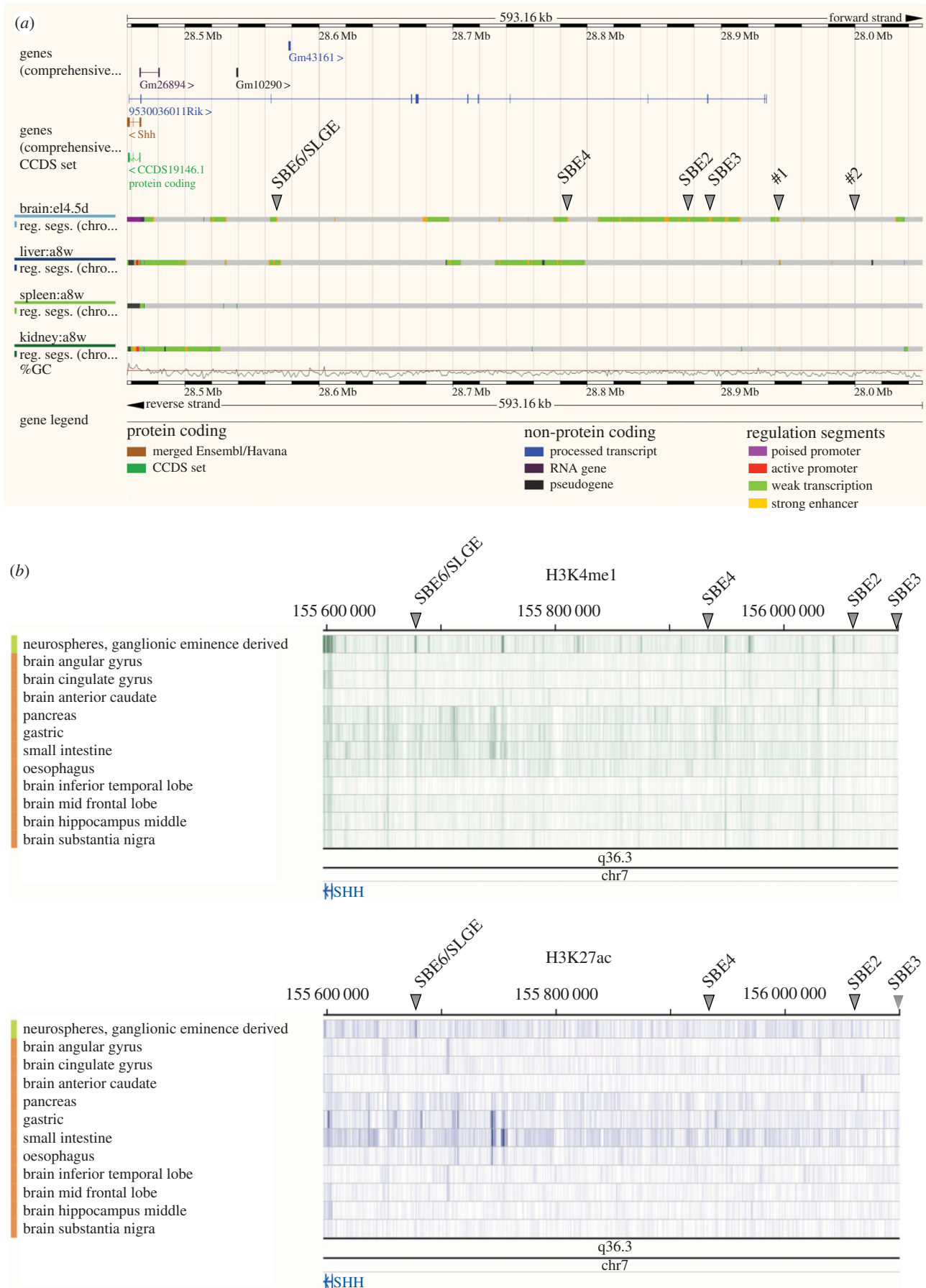


**Figure 6.** Chromatin state discovery and characterization (ChromHMM) in mouse and human *Shh* regulatory region. (a) Ensembl *Mus musculus* v. 84.38 (GRCm38.p4) view of chr5: 28 456 840–29 050 000 with regulatory feature tracks from primary cells (embryonic E14.5 brain, and adult liver, spleen and kidney) from ChromHMM. Grey arrowheads indicate previously described enhancers and two putative sequences (#1 and #2) indicated in figure 3. The position of SLGE/SBE6 is indicated. (b) Roadmap epigenome browser view of the human *Shh* locus on Hg19 (chr7: 155 595 558–156 100 554), showing H3K4me1 (top) and H3K27ac (bottom tracks) ChIP-seq from a variety of brain regions, including neurospheres, as well as pancreas, gastric, small intestine, oesophagus, tissues. Arrowheads indicate the corresponding positions of SLGE/SBE6, SBE4, SBE2 and SBE3.

sequences required for enhancer function work as assemblies of transcription factor motifs [13]. SBE6.1 and SLGE motifs may be intermingled but still specific to a precise tissue and stage of development, or may be overlapping to various extents. There are several other examples of regulatory elements capable of driving expression at multiple sites during development—for example, the global control region 5' of *HoxD* contains regulatory information capable of driving expression in the CNS and in the limb [41]. Moreover, for *SOX9* and *PAX6*, there are *cis*-regulatory elements driving expression in multiple developmental sites, and in which disease-associated variants have been identified that ablate enhancer function in one tissue but leave the other sites of expression unaltered [27,42]. Further analysis will be necessary to determine the critical transcription factor binding sites in SBE6.1/SLGE needed to drive enhancer function in different developmental settings.

**Data accessibility.** H3K4me1 and H3K27ac ChIP-on-chip data is deposited in the GEO repository (<http://www.ncbi.nlm.nih.gov/geo/>; accession no. GSE84168).

**Authors' contributions.** N.S.B. conducted most of the experiments and data analysis, prepared the figures and wrote the manuscript. P.G. conducted the bioinformatics analysis of SBE6 sequences. B.H.-B. conducted the chromatin immunoprecipitation experiments. L.A.L. assisted with the transient mouse transgenics. S.B. assisted with the study design, the zebrafish and mouse transgenics and writing of the manuscript. W.A.B. conceived of the study, designed the study, coordinated the study and helped draft and revise the manuscript. All authors gave final approval for publication.

**Competing interests.** The authors declare that they have no competing interests.

**Funding.** This work was supported by a PhD studentship to N.S.B. supported through a grant from the UK Medical Research Council to the Edinburgh Super Resolution Imaging Consortium (ESRIC). Work in the group of W.A.B is supported by an MRC University Unit grant to the MRC HGU and S.B. is supported by a CRF Biomedical Research fellowship from the Royal Society of Edinburgh.

**Acknowledgements.** We thank the staff of the MRC HGU zebrafish facility for the fish transgenics, Paul Devenney, David Read and the CBS-IGMM transgenic facility for help with the mouse transgenics, and the IGMM FACS and imaging facilities for invaluable technical help. We thank Graeme Grimes for help with microarray data processing. We thank Andy McMahon for the *Shh* probe.

## References

- Shlyueva D, Stampfel G, Stark A. 2014 Transcriptional enhancers: from properties to genome-wide predictions. *Nat. Rev. Genet.* **15**, 272–286. (doi:10.1038/nrg3682)
- Riddle RD, Johnson RL, Laufer E, Tabin C. 1993 Sonic hedgehog mediates the polarizing activity of the ZPA. *Cell* **75**, 1401–1416. (doi:10.1016/0092-8674(93)90626-2)
- McMahon AP, Ingham PW, Tabin CJ. 2003 1 Developmental roles and clinical significance of hedgehog signaling. *Curr. Top. Dev. Biol.* **53**, 1–114. (doi:10.1016/S0070-2153(03)53002-2)
- Dessaud E, McMahon AP, Briscoe J. 2008 Pattern formation in the vertebrate neural tube: a sonic hedgehog morphogen-regulated transcriptional network. *Development* **135**, 2489–2503. (doi:10.1242/dev.009324)
- Epstein DJ, McMahon AP, Joyner AL. 1999 Regionalization of Sonic hedgehog transcription along the anteroposterior axis of the mouse central nervous system is regulated by Hnf3-dependent and -independent mechanisms. *Development* **126**, 281–292.
- Jeong Y, Epstein DJ. 2003 Distinct regulators of *Shh* transcription in the floor plate and notochord indicate separate origins for these tissues in the mouse node. *Development* **130**, 3891–3902. (doi:10.1242/dev.00590)
- Jeong Y, El-Jaick K, Roessler E, Muenke M, Epstein DJ. 2006 A functional screen for sonic hedgehog regulatory elements across a 1 Mb interval identifies long-range ventral forebrain enhancers. *Development* **133**, 761–772. (doi:10.1242/dev.02239)
- Lettice LA *et al.* 2002 Disruption of a long-range *cis*-acting regulator for *Shh* causes preaxial polydactyly. *Proc. Natl Acad. Sci. USA* **99**, 7548–7553. (doi:10.1073/pnas.112212199)
- Lettice LA *et al.* 2003 A long-range *Shh* enhancer regulates expression in the developing limb and fin and is associated with preaxial polydactyly. *Hum. Mol. Genet.* **12**, 1725–1735. (doi:10.1093/hmg/ddg180)
- Sagai T, Masuya H, Tamura M, Shimizu K, Yada Y, Wakana S, Gondo Y, Noda T, Shiroishi T. 2004 Phylogenetic conservation of a limb-specific, *cis*-acting regulator of sonic hedgehog (*Shh*). *Mamm. Genome* **15**, 23–34. (doi:10.1007/s00335-033-2317-5)
- Sagai T, Amano T, Tamura M, Mizushima Y, Sumiyama K, Shiroishi T. 2009 A cluster of three long-range enhancers directs regional *Shh* expression in the epithelial linings. *Development* **136**, 1665–1674. (doi:10.1242/dev.032714)
- Anderson E, Hill RE. 2014 Long range regulation of the sonic hedgehog gene. *Curr. Opin. Genet. Dev.* **27**, 54–59. (doi:10.1016/j.gde.2014.03.011)
- Yao Y *et al.* 2016 *Cis*-regulatory architecture of a brain signaling center predates the origin of chordates. *Nat. Genet.* **48**, 575–580. (doi:10.1038/ng.3542)
- Belloni E *et al.* 1996 Identification of sonic hedgehog as a candidate gene responsible for holoprosencephaly. *Nat. Genet.* **14**, 353–356. (doi:10.1038/ng1196-353)
- Dubourg C, Bendavid C, Pasquier L, Henry C, Odent S, David V. 2007 Holoprosencephaly. *Orphanet J. Rare Dis.* **2**, 8. (doi:10.1186/1750-1172-2-8)
- Jeong Y *et al.* 2008 Regulation of a remote *Shh* forebrain enhancer by the *Six3* homeoprotein. *Nat. Genet.* **40**, 1348–1353. (doi:10.1038/ng.230)
- Ying Q-L, Stavridis M, Griffiths D, Li M, Smith A. 2003 Conversion of embryonic stem cells into neuroectodermal precursors in adherent monoculture. *Nat. Biotechnol.* **21**, 183–186. (doi:10.1038/nbt780)
- Taylor GCA, Eskeland R, Hekimoglu-Balkan B, Pradeepa MM, Bickmore WA. 2013 H4K16 acetylation marks active genes and enhancers of embryonic stem cells, but does not alter chromatin compaction. *Genome Res.* **23**, 2053–2065. (doi:10.1101/gr.155028.113)
- Therizols P, Illingworth RS, Courilleau C, Boyle S, Wood AJ, Bickmore WA. 2014 Chromatin decondensation is sufficient to alter nuclear organization in embryonic stem cells. *Science* **346**, 1238–1242. (doi:10.1126/science.1259587)
- Gilbert N, Boyle S, Sutherland H, de Las Heras J, Allan J, Jenuwein T, Bickmore WA. 2003 Formation of facultative heterochromatin in the absence of HP1. *EMBO J.* **22**, 5540–5550. (doi:10.1093/emboj/cdg520)
- Eskeland R *et al.* 2010 Ring1B compacts chromatin structure and represses gene expression independent of histone ubiquitination. *Mol. Cell* **38**, 452–464. (doi:10.1016/j.molcel.2010.02.032)
- Pradeepa MM, Sutherland HG, Ule J, Grimes GR, Bickmore WA. 2012 Psp1/Ledgf p52 binds methylated histone H3K36 and splicing factors and contributes to the regulation of alternative splicing. *PLoS Genet.* **8**, e1002717. (doi:10.1371/journal.pgen.1002717)
- Kent WJ, Sugnet CW, Furey TS, Roskin KM, Pringle TH, Zahler AM, Haussler D. 2002 The human genome browser at UCSC. *Genome Res.* **12**, 996–1006. (doi:10.1101/gr.229102)
- Loots GG, Ovcharenko I, Pachter L, Dubchak I, Rubin EM. 2002 rVista for comparative sequence-based discovery of functional transcription factor binding sites. *Genome Res.* **12**, 832–839. (doi:10.1101/gr.225502)
- Nord AS, Pattabiraman K, Visel A, Rubenstein JLR. 2015 Genomic perspectives of transcriptional

- regulation in forebrain development. *Neuron* **85**, 27–47. (doi:10.1016/j.neuron.2014.11.011)
26. Mathelier A *et al.* 2016 JASPAR 2016: a major expansion and update of the open-access database of transcription factor binding profiles. *Nucleic Acids Res.* **44**, D110–D115. (doi:10.1093/nar/gkv1176)
  27. Bhatia S *et al.* 2015 Functional assessment of disease-associated regulatory variants *in vivo* using a versatile dual colour transgenesis strategy in zebrafish. *PLoS Genet.* **11**, e1005193. (doi:10.1371/journal.pgen.1005193)
  28. Ravi V *et al.* 2013 Sequencing of Pax6 loci from the elephant shark reveals a family of Pax6 genes in vertebrate genomes, forged by ancient duplications and divergences. *PLoS Genet.* **9**, e1003177. (doi:10.1371/journal.pgen.1003177)
  29. Thisse C, Thisse B. 2008 High-resolution *in situ* hybridization to whole-mount zebrafish embryos. *Nat. Protoc.* **3**, 59–69. (doi:10.1038/nprot.2007.514)
  30. Hecksher-Sørensen J, Hill RE, Lettice L. 1998 Double labeling for whole-mount *in situ* hybridization in mouse. *Biotechniques* **24**, 914–916, 918.
  31. Echelard Y, Epstein DJ, St-Jacques B, Shen L, Mohler J, McMahon JA, McMahon AP. 1993 Sonic hedgehog, a member of a family of putative signaling molecules, is implicated in the regulation of CNS polarity. *Cell* **75**, 1417–1430. (doi:10.1016/0092-8674(93)90627-3)
  32. Cong L *et al.* 2013 Multiplex genome engineering using CRISPR/Cas systems. *Science* **339**, 819–823. (doi:10.1126/science.1231143)
  33. Ran FA *et al.* 2013 Double nicking by RNA-guided CRISPR Cas9 for enhanced genome editing specificity. *Cell* **154**, 1380–1389. (doi:10.1016/j.cell.2013.08.021)
  34. Ran FA, Hsu PD, Wright J, Agarwala V, Scott DA, Zhang F. 2013 Genome engineering using the CRISPR-Cas9 system. *Nat. Protoc.* **8**, 2281–2308. (doi:10.1038/nprot.2013.143)
  35. Pollard SM, Benchoua A, Lowell S. 2006 Neural stem cells, neurons, and glia. *Methods Enzymol.* **418**, 151–169. (doi:10.1016/S0076-6879(06)18010-6)
  36. Abranches E, Silva M, Pradier L, Schulz H, Hummel O, Henrique D, Bekman E. 2009 Neural differentiation of embryonic stem cells *in vitro*: a road map to neurogenesis in the embryo. *PLoS ONE* **4**, e6286. (doi:10.1371/journal.pone.0006286)
  37. Calo E, Wysocka J. 2013 Modification of enhancer chromatin: what, how, and why? *Mol. Cell* **49**, 825–837. (doi:10.1016/j.molcel.2013.01.038)
  38. Bonn S *et al.* 2012 Tissue-specific analysis of chromatin state identifies temporal signatures of enhancer activity during embryonic development. *Nat. Genet.* **44**, 148–156. (doi:10.1038/ng.1064)
  39. Pradeepa MM, Grimes GR, Kumar Y., Olley G, Taylor GCA, SchneiderR, Bickmore WA. 2016 Histone H3 globular domain acetylation identifies a new class of enhancers. *Nat. Genet.* **48**, 681–686. (doi:10.1038/ng.3550)
  40. Tsukiji N, Amano T, Shiroishi T. 2014 A novel regulatory element for Shh expression in the lung and gut of mouse embryos. *Mech. Dev.* **131**, 127–136. (doi:10.1016/j.mod.2013.09.003)
  41. Spitz F, Gonzalez F, Duboule D. 2003 A global control region defines a chromosomal regulatory landscape containing the HoxD cluster. *Cell* **113**, 405–417. (doi:10.1016/S0092-8674(03)00310-6)
  42. Bhatia S *et al.* 2013 Disruption of autoregulatory feedback by a mutation in a remote, ultraconserved PAX6 enhancer causes aniridia. *Am. J. Hum. Genet.* **93**, 1126–1134. (doi:10.1016/j.ajhg.2013.10.028)